科学通报 2019 年 第 64 卷 第 11 期: 1179 ~ 1190
论 文
《中国科学》杂志社
SCIENCE CHINA PRESS

东北平原钻孔的磁性地层定年及松嫩古湖演化

詹涛[1*], 曾方明[2], 谢远云[3], 杨业[1], 葛俊逸[4], 马永法[1], 迟云平[3], 康春国[5], 姜侠[6], 余中元[7], 张俊[1], 李峨[1], 周鑫[8]

1. 黑龙江省生态地质调查研究总院, 哈尔滨 150030;
2. 中国科学院青海盐湖研究所, 西宁 810008;
3. 哈尔滨师范大学地理科学学院, 哈尔滨 150025;
4. 中国科学院古脊椎动物与古人类研究所, 北京 100044;
5. 哈尔滨学院, 哈尔滨 150086;
6. 黑龙江省地质矿产局, 哈尔滨 150036;
7. 防灾科技学院综合减灾研究所, 三河 065201;
8. 中国科学技术大学地球和空间科学学院, 合肥 230026;
* 联系人, E-mail:hljzhantao@163.com

2018-12-06 收稿, 2019-01-21 修回, 2019-01-22 接受, 2019-03-25 网络版发表
国家自然科学基金(41301040, 41601200)、黑龙江省国土资源科研类项目(201407)和国土资源部公益性科研专项(201311137)资助

摘要 中国东北平原第四纪湖相沉积物是记录中纬度东亚季风和气候环境变化的理想载体. 然而, 目前关于该套湖相沉积地层尚缺乏高分辨率地层学和高精度的年代学研究, 从而限制了对该区气候环境变化机理的理解. 本研究重建了东北平原乾安令字(Qiananlingzi, QAL)孔的高分辨率磁化率地层, 并对该套沉积进行了系统的古地磁和光释光年代学研究. 结果显示, QAL钻孔记录了Olduvai正极性亚时以来的沉积. 沉积物磁化率变化存在轨道时间尺度上的变化, 粗颗粒的粉砂层一般呈现磁化率低值, 细颗粒的黏土层一般呈现高值, 岩石磁学参数表明磁化率低值层位高矫顽力硬磁性矿物贡献大, 高值层位低矫顽力软磁性矿物贡献大; 该套湖相地层的沉积年代约为1180~450 ka, 历时约730 ka, 松嫩古湖的几近消失可能与依舒断裂导致的多次沉降使得松花江将松嫩古湖湖水泄于三江平原有关. 基于本文详细的磁化率地层和高精度的年代学结果, 该湖相沉积有望成为解译中纬度中亚区域中更新世轨道时间尺度古气候变化的理想材料.

关键词 东北平原, 松嫩古湖, 磁性地层, 光释光, 磁化率

湖泊沉积是古气候、古环境变化研究的重要载体, 因其分布广泛, 在全球气候变化的区域响应研究方面独具优势[1,2], 被广泛应用于恢复新生代以来构造[3~5]、轨道[6,7]和千-百年[8~10]时间尺度古气候环境变化研究, 尤其在恢复第四纪不同时间尺度上古气候环境演化方面取得大量成果[11~17].

东北平原位于我国东部季风区北部, 纬度较高, 对冰量等高纬度信号反应敏感; 同时, 受到低纬气候(如东亚夏季风)的显著影响, 是研究高低纬相互作用的理想区域. 已有研究发现, 在早-中更新世时期, 东北平原存在一个面积约为50000 km^{2}的大湖, 晚更新世干涸[18~20], 该套湖相沉积地层是研究第四纪时期古气候环境变化的良好载体. 针对该套沉积物, 已开展过古地磁[19,20]、黏土矿物学[20]和孢粉[20,21]等研究, 认定该套

引用格式: 詹涛, 曾方明, 谢远云, 等. 东北平原钻孔的磁性地层定年及松嫩古湖演化. 科学通报, 2019, 64: 1179–1190
Zhan T, Zeng F M, Xie Y Y, et al. Magnetostratigraphic dating of a drill core from the Northeast Plain of China: Implications for the evolution of Songnen paleo-lake (in Chinese). Chin Sci Bull, 2019, 64: 1179–1190, doi: 10.1360/N972018-01212

地层起始于早更新世[20]，为静水环境下的淡水沉积[20]，并进行了孢粉带划分[20,21]．然而囿于当时的研究条件，在以下方面还存在着一些不足：(1) 过去针对该套地层进行的古地磁年代学研究较粗略，且缺乏岩石磁学的辅助论证；(2) 过去的研究只是对地层的宏观控制，缺乏高精度年代学和高分辨率环境替代指标的研究，尤其轨道尺度上的研究尚未开展．

针对上述问题，我们对东北平原腹地乾安令字(Qiananlingzi，QAL)钻孔开展高分辨率的古地磁和光释光(optically stimulated luminescence，OSL)年代学研究，以期建立较为准确的年代框架，并开展高分辨率的磁化率地层研究，用于判断地层精细变化，为后续开展地层对比和建立高分辨率的环境变化序列提供年代学和气候环境指标基础．

1 材料和方法

东北平原也称松辽平原，松辽分水岭以南为辽河平原，以北为松嫩平原，位于我国东北季风区中部(图1)，西与大兴安岭接壤，东北与小兴安岭紧邻，东南为长白山山脉．东北平原地区沉积了巨厚的侏罗纪-白垩纪地层和420~530 m厚的古近纪-新近纪地层，以及75~200 m厚的第四纪地层[20]．

QAL钻孔(44°49′04″N，123°48′46″E)位于吉林省乾安县城西南约50 km，处于东北平原腹地，是过去研究认为的第四纪松嫩古大湖中心位置[18~20]．2015年9月我们采用双管单动内衬塑料套管钻探取心技术，获得岩心120.54 m．本次研究重点针对上部80 m以细颗粒为主岩心沉积物，该部分岩心采取率达到92%．为了避免岩心样品曝光的风险，在岩心孔位边上人工挖掘剖面，进行同层位OSL样品采集，将直径约5 cm、长约30 cm的钢管打入地层之中，拔出钢管后迅速将两端用黑塑料袋包裹紧密，送实验室进行测年．

古地磁取样间距为40 cm，共188个，代表约23个沉积层位．对于胶结好的定向样品加工成边长为2 cm的立方体，而对于胶结弱的样品采用边长为2 cm的无磁塑料盒取样．剩磁测量采用安装在零磁空间(＜300 nT)的2G760三轴超导磁力仪上完成．对QAL钻孔的188个样品进行系统的交变退磁，采用16步退磁(不含天然剩磁，natural remanent magnetization，NRM)，最大退磁场强度为80 mT，间隔2.5~10 mT．

磁化率样品测试间距为10 cm，共796个，用捷克Agico公司生产的KLY-3卡帕桥磁化率仪测量．在典型

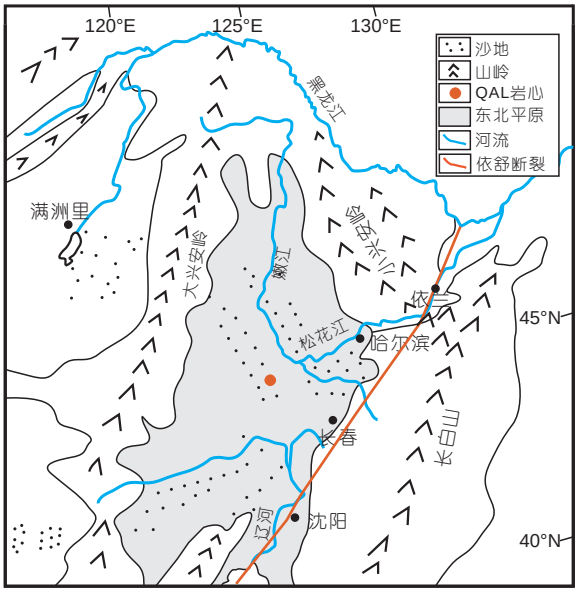

图 1 东北平原QAL钻孔的地理位置

Figure 1 Location of the QAL Core in the Northeast Plain

代表层位选取3个样品进行磁化率随温度变化曲线(χ-T)测量和磁滞参数测量．磁滞参数(包括饱和剩余磁化强度M_{rs}、饱和磁化强度M_s、矫顽力B_c和剩磁矫顽力B_{cr})、等温剩磁(isothermal remanent magnetization，IRM)获得曲线及其在反向场中的退磁曲线用美国普林斯顿仪器公司生产的MicroMag 3900型振动样品磁力仪测量．磁化率随温度变化曲线(χ-T)用捷克Agico公司生产的KLY-3卡帕桥磁化率仪测量．取粉末样品约200 mg，研磨后装入玻璃样品管，设定温度区间为40~700℃，在加热过程中连续测量样品的磁化率，之后从700℃降温至40℃，并测量样品的磁化率．为了避免样品在加热过程中氧化，实验过程在氩气环境中进行．系统使用频率为875 Hz，温度控制系统为CS-3，温度传感器为CS TEMPM1，精度为±2℃，加热速率为9℃/min．磁学实验均在中国科学院地质与地球物理研究所完成．

对于OSL年龄测试，在暗室环境下将两端样品取出，用来测含水率以及剂量率，其余样品进行等效剂量测试分析．取5~10 g已烘干的样品，用玛瑙研钵研磨300目以下，于北京中国原子能科学研究院利用中子活化法测量样品中U，Th和K的含量，计算剂量率．暗室环境下，用湿筛法筛分得到90~150 μm组分并放入烘箱中50℃烘干．将烘干样品放入烧杯中，加入30%分析H_2O_2除去有机质，用HCl去除碳酸盐，然后用纯水将样品清洗多次至中性后，放入烘箱中烘干．利用密度为

2.62~2.70 g/cm^{3}的重液，提取样品中的石英颗粒．用40%的HF刻蚀石英矿物颗粒60 min，以除去残留的长石以及石英矿物表层受α粒子影响的部分，之后用10%稀盐酸洗去残留的氟化物．使用2 mm小片法进行等效剂量测试, 测试仪器为Risø TL/OSL DA-20型全自动释光仪, 配置EMI 9235 QA光电倍增管, 红外光源波长为850 nm，蓝光光源波长为470 nm，激发功率约为50 mW/cm^2，设置效率为90%，滤光片为厚度是7.5 mm的U-340．人工剂量辐照为仪器内置的^{90}Sr/^{90}Y放射源, 放射源的剂量率为0.1031 Gy/s．测试流程为标准的单片再生剂量(SAR)法[22,23], 详见表1. 以上实验在中国科学院古脊椎动物与古人类研究所完成.

2 结果

2.1 岩性与磁化率地层

QAL钻孔沉积物岩性特征自下而上可划分为三段[18]或四段[19]. 按前者标准, 沉积物自下而上可划分为白土山组、大青沟组和黄土状土．鉴于白土山组地层各处成因不一，后者将此处白土山地层更名为“乾安组”, 将大青沟组分为两段, 上段命名为“林甸组”, 下段命名为“令字组”．因后者划分更为细致，本文采用4段划分法(图2).

乾安组(80~71 m深)：黄绿、棕红和灰棕色粉细砂为主, 夹棕黑色粉质黏土，下部为砾石层，为河流相沉积环境．该套地层磁化率整体呈现高值，变化范围为(11.2~104)×10^{-8} m^3 kg^{-1}, 平均值为36.9×10^{-8} m^3 kg^{-1}.

令字组(71~44 m深)和林甸组(44~19.5 m深)为灰绿色黏土与灰白色粉砂互层, 含贝壳化石, 为湖泊沉积环境．该套地层的磁化率整体偏低，变化范围为(3.19~38.2)×10^{-8} m^3 kg^{-1}，平均值为13.0×10^{-8} m^3 kg^{-1}．粗颗粒粉砂层磁化率一般呈现低值，细颗粒黏土层一般呈现高值.

黄土状土(19.5~0 m深)：该段含灰白色粉砂，棕黑色黏土层位, 但较多层位出现棕黄色黏土质粉砂层. 从沉积相分析该段的沉积环境表明湖泊大面积缩小，并存在几近干涸的时期，有风成黄土和二次搬运的黄土状土出现．该套地层磁化率整体较下伏湖相地层稍高, 变化范围为(4.05~35.8)×10^{-8} m^3 kg^{-1}，平均值为15.4×10^{-8} m^3 kg^{-1}.

2.2 岩石磁学

图3中左侧图是各个地层中代表性样品的磁滞回线, 其中黑色线代表顺磁矫正后的曲线, 矫正后的曲线有很大变化, 说明顺磁性矿物有很大贡献. 磁化率较高的样品矫正后的曲线大部分在300 mT之后接近闭合, 说明沉积物中以软磁性矿物为主(图3(a), (c), 而磁化率较低的样品在500 mT仍未饱和(图3(b), (d)), 且出现了“细腰”现象，说明样品中存在高、低矫顽力的磁性矿物, 并且高矫顽力磁性矿物含量相对较高. 高磁化率地层样品IRM获得曲线显示外加场为300 mT的时候，饱和等温剩磁获得达到90%, 说明地层中以软磁性矿物为主, 而低磁化率地层样品外加场为300 mT的时候, 仅获得饱和等温剩磁的70%，说明硬磁性矿物的贡献很大, 反向场退磁曲线呈现的情况也很一致.

磁化率随温度变化曲线是判断沉积物中磁性矿物种类的一种常用手段[24,25]. 从图4(a), (c)中可以看出, 样品加热到580℃左右，磁化率值急剧降低，表明磁铁矿是磁化率的主要贡献者．在降温过程中磁化率值在580℃(即磁铁矿居里点)附近急剧上升，说明新生成的

表 1 OSL测年样品测试程序

Table 1 Testing procedure for optically stimulated luminescence

步骤	操作	说明
1	辐照剂量i为循环数(i=0, 1, 2, 3)	当i=0为天然剂量(不辐照)
2	预热280℃, 10 s	去除热不稳定信号
3	蓝光激发, 激发温度125℃	获得OSL信号
4	辐照实验剂量	用以校正释光感量变化
5	预热220℃, 时间0 s	去除热不稳定信号
6	蓝光激发, 激发温度为125℃	获得实验剂量的OSL响应
7	280℃下激发测片	消除可能的OSL信号积累

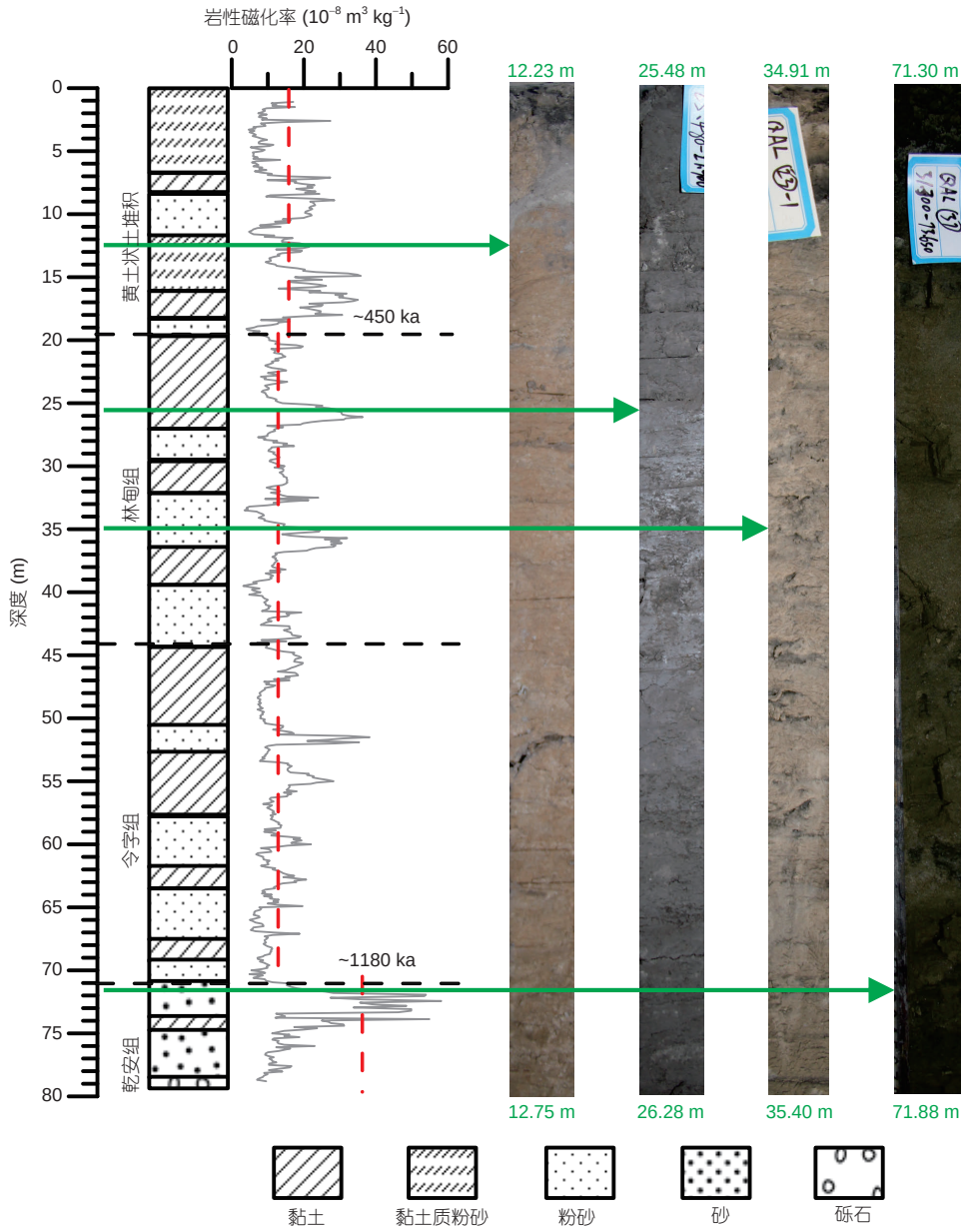

图 2 QAL钻孔的岩性柱、磁化率和岩心照片. 黑色虚线表示各组界线, 红色虚线表示各组磁化率的平均值

Figure 2 Lithology, magnetic susceptibility and photos of QAL core. The black dashed line represents the boundary of each formation. The red dashed line represents the average value of magnetic susceptibility in each formation

磁性矿物还是以磁铁矿为主. 而图4(b), (d)沉积物加热到580℃以后仍有下降, 显示了赤铁矿的存在, 与岩石磁学反映的高低矫顽力磁性矿物同时存在的结果一致.

2.3 OSL

利用早期背景值扣除法对结果进行分析. 使用通道1~2(0~0.32 s)作为快组分信号区间, 通道3~7(0.32~1.12 s)作为背景信号区间获得等效剂量值. 每个样品都测试8个有效数据, 然后用测得的平均值代表该样品的等效剂量. 利用中子活化法测得的U, Th以及K的数据, 然后利用Hutnly剂量率计算表格计算, 输入经纬度海拔等进行校正, 含水率按照实测结果, 误差给定5%. 粗颗粒石英(90~150 μm)的OSL信号在前2 s快速衰减, 表明粗颗粒石英OSL信号是以快组分为主导, 据此可以根据指数拟合建立再生曲线. QAL钻孔1.4 m深度以上地层测年结果如表2, 1.4 m深处的年龄为~50 ka.

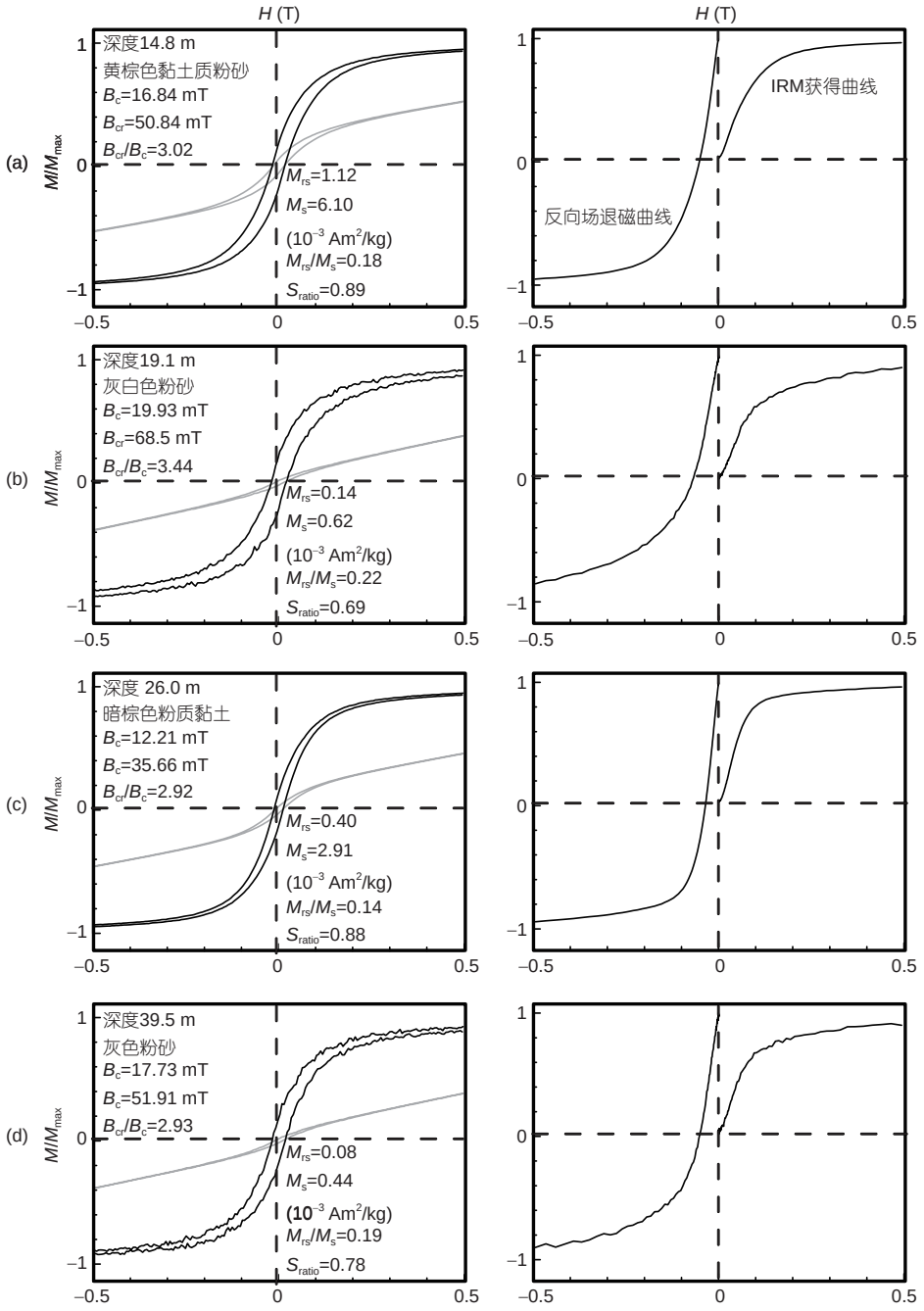

图 3 QAL钻孔代表层位样品的磁滞回线. (a), (c) 位于高磁化率值层位; (b), (d) 位于低磁化率值层位. 灰色线代表原始曲线, 黑色线代表顺磁矫正后的曲线(左), IRM获得曲线和反向场退磁曲线(右)

Figure 3 Magnetic hysteresis loops. (a), (c) The samples in higher MS layer; (b), (d) the samples in low MS Layer. The grey line represents the original curve and the black line represents the paramagnetic corrected curve (left). IRM acquisition curves and demagnetization curves (right) for representative samples from QAL core

2.4 古地磁

典型样品的系统退磁结果的正交投影见图5, 交变退磁一般在15或20 mT就去掉次生剩磁, 获得特征剩磁. 大部分样品, 在40~80 mT区间内(图5)就获得稳定的特征剩磁方向. 以最大角偏差小于15°为界限, 共79个样品获得稳定的特征剩磁方向, 占总样品数的43%, 并且依据连续3个以上相同极性的样品可定义为同一

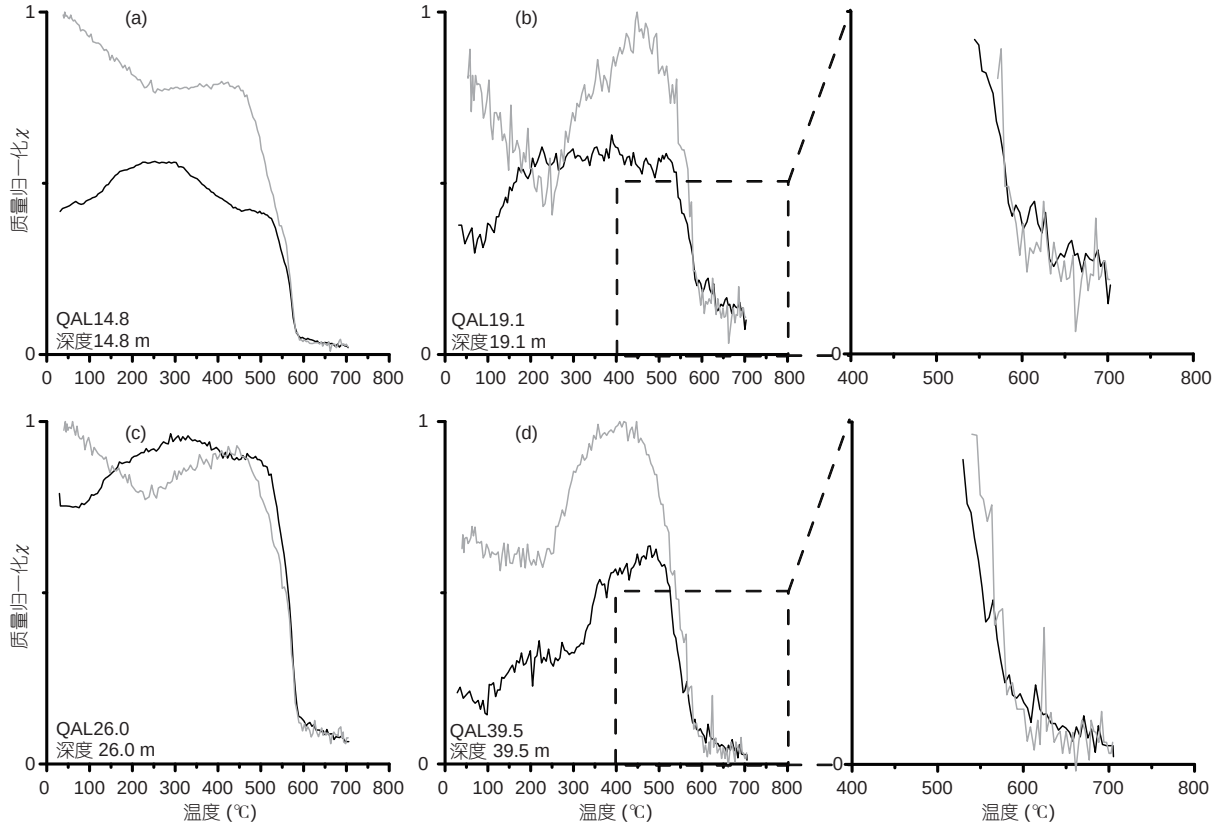

图 4 QAL钻孔代表性样品的磁化率随温度变化曲线. (a), (c) 位于高磁化率值层位; (b), (d) 位于低磁化率值层位. 黑色线表示加热曲线, 灰色线代表冷却曲线

Figure 4 High-temperature magnetic susceptibility (χ-T) for selected specimens of QAL core. (a), (c) The samples in higher MS layer; (b), (d) the samples in low MS layer. The black line represents the heating curve, and the gray line represents the cooling zone curve

表 2 QAL钻孔岩心上部地层OSL测年结果

Table 2 OSL dating results of the upper strata of QAL core

样品号	深度(m)	U(ppm)	Th(ppm)	K(%)	含水量(%)	剂量率(Gy/ka)	等效剂量(Gy)	年龄(ka)
HED300	0.2	2.42±0.1	8.60±0.27	2.52±0.07	2.62±5	3.40±0.24	4.78±0.68	1.41±0.22
HED301	0.4	1.43±0.07	10.00±0.46	2.48±0.07	9.61±5	3.25±0.23	24.49±4.07	7.53±1.36
HED302	0.6	1.36±0.07	9.84±0.23	2.29±0.07	11.47±5	3.21±0.23	49.01±4.53	15.27±1.78
HED303	0.8	1.74±0.08	8.75±0.22	2.16±0.07	9.85±5	2.84±0.20	43.92±1.58	15.44±1.21
HED304	1.0	1.53±0.07	7.71±0.23	2.51±0.07	11.29±5	3.09±0.22	131.06±9.17	42.42±4.24
HED305	1.2	2.42±0.1	8.60±0.27	2.52±0.07	11.97±5	3.37±0.24	145.58±8.68	43.24±3.83
HED306	1.4	1.43±0.07	8.50±0.46	2.48±0.07	6.23±5	3.13±0.22	157.39±5.07	50.32±1.71

个极性带的原则, 鉴于钻孔样品磁偏角的随机性, 仅利用磁倾角建立QAL钻孔的磁极性倒转序列(图6).

QAL钻孔记录了5个极性带, 包括3个正极性带和2个负极性带. 其中0~34.7 m为正极性N1, 34.7~54.0 m为负极性R1, 54.0~61.4 m为正极性N2, 61.4~74.6 m为负极性R2, 74.6~78.0 m为正极性N3.

3 讨论

3.1 QAL钻孔磁化率变化的初步分析

磁化率是代表磁性矿物多少的指标, 在黄土高原黄土-古土壤序列里面能够体现成壤强度, 进而反映季风降水的多少[27~30], 但在河湖相沉积物里面的环境指

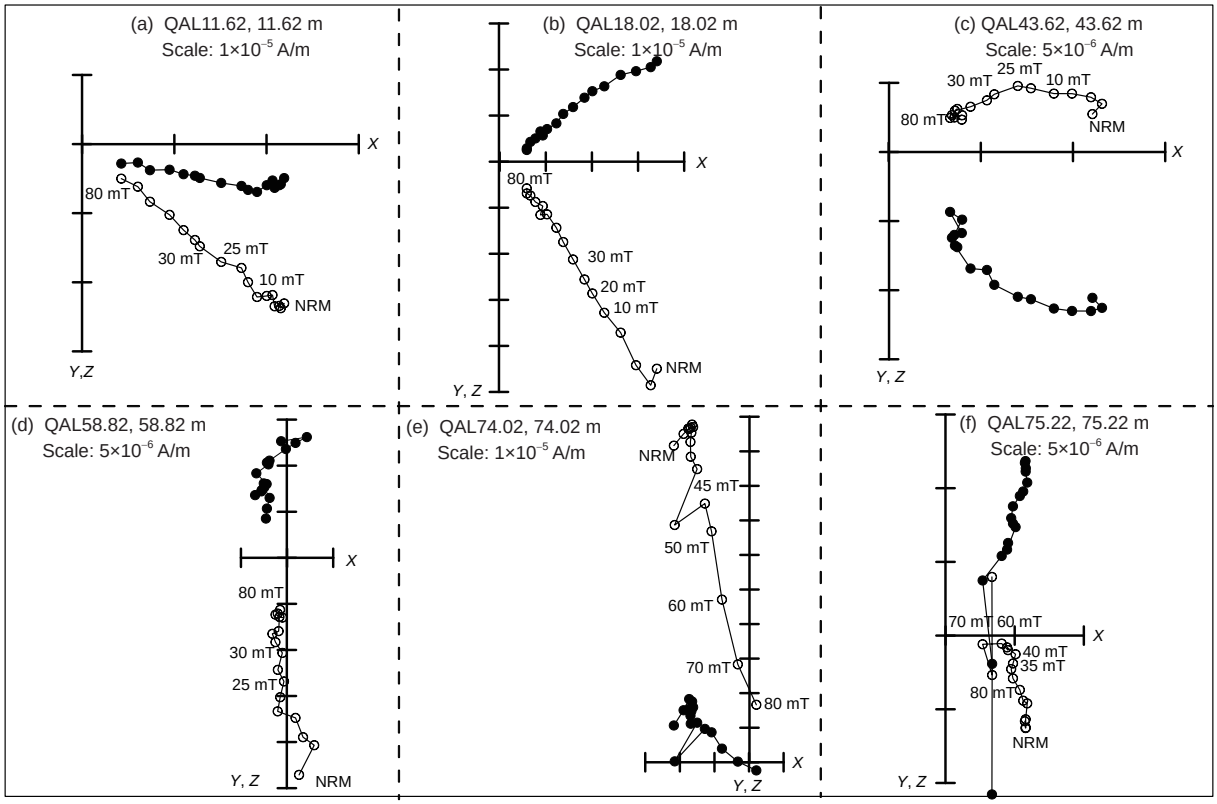

图 5 QAL钻孔代表性样品的退磁矢量图. 实心(空心)圆代表水平分量(垂直分量), NRM表示天然剩磁
Figure 5 Orthogonal demagnetization diagrams of typical samples from QAL core. Solid (open) circles represent the projections on the horizontal (vertical) plane. The numbers refer to alternating fields in mT. NRM is the natural remanent magnetization

示意义较为复杂[31]. 乾安组上部河流相地层沉积时期, 可能对应了氧化为主的环境, 保存了较多的强磁性矿物, 造成磁化率呈现高值. 令字组和林甸组对应湖泊环境, 主体的还原环境可能导致其整体强磁性矿物含量较低, 磁化率整体较低, 大多数黏土层较粉砂层呈现较高值, 结合后面的年代学研究, 呈现的是轨道尺度上的波动. 上部的黄土状土地层出现的时期, 代表湖泊大幅度萎缩, 主体氧化环境出现, 并且黄土状土中强磁性矿物含量较高, 因而其磁化率明显高于下伏湖相地层. 磁滞回线和磁化率随温度变化曲线结果表明磁化率低值层位高矫顽力硬磁性矿物贡献大, 高值层位低矫顽力软磁性矿物贡献大. 以上地层磁化率的变化原因及环境指代意义, 需未来进行详细的环境磁学指标和岩石磁学进行综合解译[31].

3.2 第四纪松嫩古湖演化及驱动因素

3.2.1 QAL钻孔磁极性序列与地磁极性年表的对比

与地磁极性年表进行对比(图6), 将上部最长的正极性N1对应于布容(Brunhes)正极性时, R1~N3以负极性为主的极性段对应于松山(Matuyama)负极性时, 其中N2对应于Jaramillo正极性亚时, N3对应于Olduvai正极性亚时, 布容/松山地磁极性倒转(即B/M界线)位于34.7 m. 以上结果与前人对该区钻孔开展过的研究基本一致[19]. 鉴于Olduvai正极性亚时处于乾安组地层中, 岩性为粉细砂夹粉质黏土、含砾中粗砂, 为河流相的冲、洪积物, 河流相沉积物往往分布局限, 容易造成地层的缺失, 沉积速率变化较大, 令字组的底界年龄, 采用R1＋N2段沉积速率的线性外推获得.

3.2.2 古大湖的起始和大幅度萎缩或消失年代

通过OSL测年和古地磁极性倒转界线年龄控制点, 得到QAL钻孔沉积地层深度和年龄的关系(图7), 进而可获得古湖存在的大致年龄范围. 从图中可以看出两个沉积速率变化较大处: (1) 在0.8~1 m深段沉积速率较低, OSL年龄从15.44±1.21 ka增加至42.42±4.24 ka, 沉积速率降至0.74 cm/ka, 该阶段对应于末次冰盛期, 处于湖泊沉积、黄土状土等交错沉积时期, 而且该区

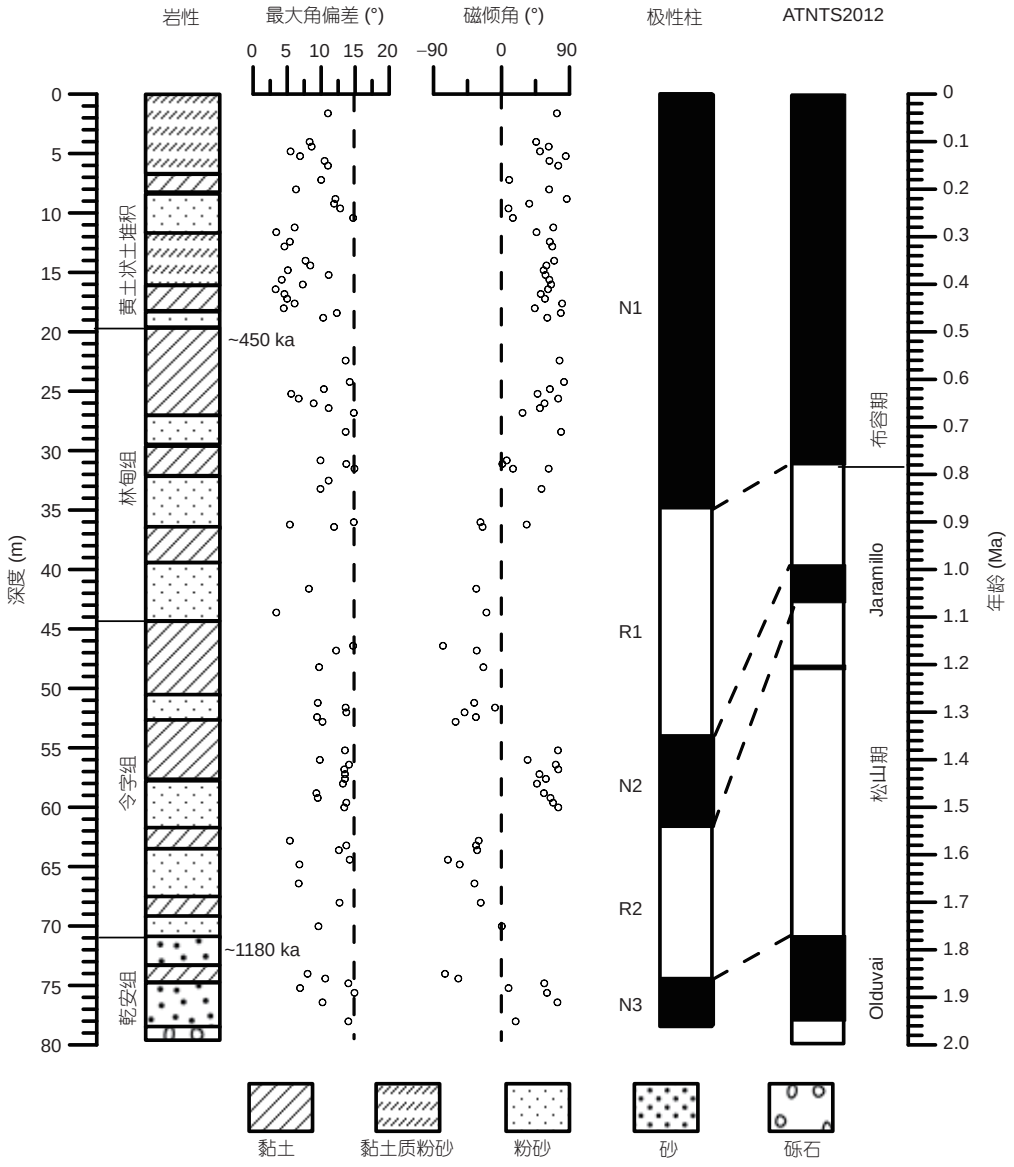

图 6 QAL钻孔的磁极性地层结果(岩性、最大角偏差、磁偏角、极性柱及其和地磁极性年表(ATNTS2012)) 的对比[26]
Figure 6 Magnetostratigraphy results of QAL core (lithology, maximum angular deviation, inclination and polarity zonation, and its correlation with the geomagnetic polarity timescale (ATNTS2012))[26]

为风成哈尔滨组的物源区[32]，风蚀作用可能造成该区地层存在万年尺度的缺失; (2) 在61.4~74.6 m深之间沉积速率也急速下降，达到1.86 cm/ka，河流相乾安组与湖相令字组界线位于该阶段，河流环境沉积不稳定造成地层的缺失, 沉积速率突变. 湖泊环境较河流环境稳定，为此，令字组底界采用R1＋N2段的沉积速率外推获得年龄比较合理, 约为1180 ka.

林甸组的顶界年龄采用1.4 m的OSL年龄50.32±1.71 ka和B/M界线年龄781.0 ka线性内插获得，即古湖几近消失的年龄约为450 ka. 综上，松嫩古湖大范围存在的时间段为中更新世晚期至晚更新世(约1180~450 ka), 历时约730 ka.

3.2.3 松嫩古湖大幅度萎缩或消失的可能驱动因素

湖泊的大幅度萎缩或消失的可能原因通常有两种: (1) 气候变干, 降水减少, 湖平面大幅度下降; (2) 构造运动导致湖盆变化, 湖水外泄.

通过对东北季风区内蒙赤峰NYZG黄土剖面粒度特征研究，Zeng等人[33]发现中更新世以来东北季风区虽有逐渐变干的趋势, 并且识别出两次干旱事件, 但分别在~650.0和~300.0 ka, 在~450 ka前后无明显变化. 另

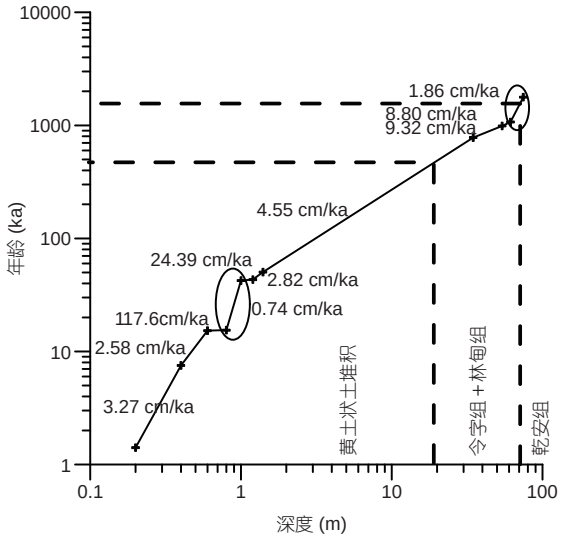

图 7 QAL钻孔深度-年龄图. 虚线表示各组地层界线, 黑色空心圈表示沉积速率突变层位

Figure 7 Diagram of depth-age for QAL core. The dashed line represents the stratigraphic boundary, and the black hollow circle represents the abrupt change of deposition rate

图 8 松嫩古湖-风成哈尔滨组耦合演化示意图

Figure 8 Schematic diagram of coupling evolution model of Songnen paleo-lake and eolian Harbin Formation

外, 在该时期前后黄土高原反映夏季风的磁化率和游离铁/全铁指标[34]都显示, 夏季风降水很可能有增强的趋势. 以上记录说明东北平原第四纪古湖的大幅度萎缩可能不是气候的原因.

初本君等人[35]曾提出, 约500.0~600.0 ka期间, 依舒断裂的多次沉降导致古松花江沟通了第四纪松嫩古湖和三江平原的水力联系, 松嫩古湖湖水泄于三江平原, 从而导致松嫩古湖几近消亡. 而裘善文等人[20]则认为古松花江的溯源侵蚀导致松嫩古大湖流向松花江的出水量加大, 导致古湖的消亡. 为此, 构造运动可能是~450 ka松嫩古湖几近消亡的原因, 但这可能需要在依兰峡谷找到依舒断裂活动和松花江古流向等更为直接的沉积学、年代学证据. 图8为依舒断裂多次沉降导致松嫩古湖-风成哈尔滨组演化耦合模式示意图, 在~450 ka之前, 松嫩平原存在一个面积约50000 km^{2}的古湖[18~20], 在~450 ka之后, 依舒断裂的多次沉降使得松花江沟通了松嫩古湖与三江平原的水力联系, 最终导致松嫩古湖的几近消亡.

4 结论与展望

本文通过对东北平原QAL钻孔开展详细的OSL和古地磁年代学研究, 并结合高分辨率的磁化率地层和岩石磁学结果, 得出以下结论, 并予以展望.

(1) 面积广阔的松嫩古湖存在于早更新世晚期至中更新世, 为约1180~450 ka期间, 历时约730 ka; 该套湖相沉积磁化率地层显示了轨道尺度的波动, 粗颗粒粉砂层磁化率一般呈现高值, 细颗粒的黏土层一般呈现低值; 高磁化率地层低矫顽力磁性矿物贡献大, 低磁化率地层高矫顽力磁性矿物贡献大.

(2) 区域及全球气候演化记录并未显示松嫩古大湖几近消失为气候变化所驱动, 而依舒断裂多次沉降使得松花江沟通了松嫩古湖与三江平原的水力联系, 导致松嫩古湖湖水泄于三江平原可能是古湖几近消失的原因.

(3) 该套湖相沉积是研究东北平原中更新世轨道尺度气候环境演化的理想记录, 未来应结合系统的环境磁学以及沉积学、地球化学等环境替代指标, 开展"中更新世转型"的区域响应及其驱动机制研究.

致谢 感谢中国科学院地质与地球物理研究所岩石圈演化国家重点实验室沈中山博士在古地磁和岩石磁学样品测试分析过程中给予的帮助.

参考文献

1 Shen J, Xue B, Wu J L, et al. Lake Sediments and Environmental Evolution (in Chinese). Beijing: Science Press, 2010 [沈吉, 薛滨, 吴敬禄, 等. 湖

泊沉积与环境演化. 北京: 科学出版社, 2010]
2 Shen J. Spatiotemporal variations of Chinese lakes and their driving mechanisms since the Last Glacial Maximum: A review and synthesis of lacustrine sediment archives. Chin Sci Bull, 2012, 57: 3228−3242 [沈吉. 末次盛冰期以来中国湖泊时空演变及驱动机制研究综述: 来自湖泊沉积的证据. 科学通报, 2012, 57: 3228–3242]
3 Dupont-Nivet G, Krijgsman W, Langereis C G, et al. Tibetan Plateau aridification linked to global cooling at the Eocene-Oligocene transition. Nature, 2007, 445: 635–638
4 Xiao G, Guo Z, Dupont-Nivet G, et al. Evidence for northeastern tibetan plateau uplift between 25 and 20 Ma in the sedimentary archive of the Xining Basin, northwestern China. Earth Planet Sci Lett, 2012, 317-318: 185–195
5 Zhang C, Guo Z. Clay mineral changes across the Eocene-Oligocene transition in the sedimentary sequence at Xining occurred prior to global cooling. Palaeogeogr Palaeoclimatol Palaeoecol, 2014, 411: 18–29
6 Xiao G Q, Abels H A, Yao Z Q, et al. Asian aridification linked to the first step of the Eocene-Oligocene climate Transition (EOT) in obliquity-dominated terrestrial records (Xining Basin, China). Clim Past, 2010, 6: 501–513
7 Nie J, Garzione C, Su Q, et al. Dominant 100000-year precipitation cyclicity in a late miocene lake from northeast tibet. Sci Adv, 2017, 3: e1600762
8 An Z, Colman S M, Zhou W, et al. Interplay between the Westerlies and Asian monsoon recorded in Lake Qinghai sediments since 32 ka. Sci Rep, 2012, 2: 619
9 Xu D, Lu H, Chu G, et al. 500-year climate cycles stacking of recent centennial warming documented in an East Asian pollen record. Sci Rep, 2014, 4: 3611
10 Liu J B, Chen F H, Chen J H, et al. Humid Medieval Warm Period recorded by magnetic characteristics of sediments from Gonghai Lake, Shanxi, North China. Chin Sci Bull, 2011, 56: 2464–2474
11 Yancheva G, Nowaczyk N R, Mingram J, et al. Influence of the intertropical convergence zone on the East Asian monsoon. Nature, 2007, 445: 74–77
12 An Z S, Clemens S C, Shen J, et al. Glacial-interglacial Indian summer monsoon dynamics. Science, 2011, 333: 719–723
13 Xiao J, Xu Q, Nakamura T, et al. Holocene vegetation variation in the Daihai Lake region of north-central China: A direct indication of the Asian monsoon climatic history. Quat Sci Rev, 2004, 23: 1669–1679
14 Ao H, Dekkers M J, Xiao G, et al. Different orbital rhythms in the Asian summer monsoon records from north and south China during the Pleistocene. Glob Planet Change, 2012, 80-81: 51–60
15 Chu G, Sun Q, Xie M, et al. Holocene cyclic climatic variations and the role of the Pacific Ocean as recorded in varved sediments from northeastern China. Quat Sci Rev, 2014, 102: 85–95
16 Zhou X, Sun L, Zhan T, et al. Time-transgressive onset of the Holocene optimum in the East Asian monsoon region. Earth Planet Sci Lett, 2016, 456: 39–46
17 Caley T, Extier T, Collins J A, et al. A two-million-year-long hydroclimatic context for hominin evolution in southeastern Africa. Nature, 2018, 560: 76–79
18 Qiu S W, Xia Y M, Li F H, et al. Mid-Quaternary paleogeography of Songliao Plain of China (in Chinese). Chin Sci Bull, 1984, 29: 172−174 [裘善文, 夏玉梅, 李凤华, 等. 松辽平原第四纪中期古地理研究. 科学通报, 1984, 29: 172−174]
19 Qiu S W, Xia Y M, Wang P F, et al. Pleistocene stratigraphy and sedimentary environment in Songliao Plain of China (in Chinese). Sci China Ser B, 1988, 4: 431−441 [裘善文, 夏玉海, 汪佩芳, 等. 松辽平原更新世地层及其沉积环境的研究. 中国科学(B辑), 1988, 4: 431−441]
20 Qiu S W, Wang X K, Zhang S Q, et al. The evolution of the large paleolake in Songliao plain and its formation (in Chinese). Quat Sci, 2012, 32: 1011−1021 [裘善文, 王锡魁, 张淑芹, 等. 松辽平原古大湖演变及其平原的形成. 第四纪研究, 2012, 32: 1011−1021]
21 Xia Y M, Wang P F. The paleobotany and paleoclimate in the Songnen plain: A study on the late Tertiary-Pleistocene spore pollen assemblages (in Chinese). Acta Geogr Sin, 1987, 42: 165−178 [夏玉梅, 汪佩芳. 松嫩平原晚第三纪—更新世孢粉组合及古植被与古气候的研究. 地理学报, 1987, 42: 165−178]
22 Murray A S, Wintle A G. Luminescence dating of quartz using an improved single-aliquot regenerative-dose protocol. Radiat Meas, 2000, 32: 57–73
23 Murray A S, Wintle A G. The single aliquot regenerative dose protocol: Potential for improvements in reliability. Radiat Meas, 2003, 37: 377–381
24 Deng C, Zhu R, Verosub K L, et al. Paleoclimatic significance of the temperature-dependent susceptibility of holocene loess along a NW-SE transect in the Chinese Loess Plateau. Geophys Res Lett, 2000, 27: 3715–3718
25 Deng C, Zhu R, Jackson M J, et al. Variability of the temperature-dependent susceptibility of the Holocene eolian deposits in the Chinese Loess Plateau: A pedogenesis indicator. Phys Chem Earth A, 2001, 26: 873–878
26 Hilgen F J, Lourens L J, Van Dam J A. The neogene period. In: Gradstein F M, Ogg J G, Schmitz M D, et al., eds. The Geologic Time Scale 2012. Amsterdam: Elsevier BV, 2012, 2: 923–978

27 Zhou L P, Oldfield F, Wintle A G, et al. Partly pedogenic origin of magnetic variations in Chinese loess. Nature, 1990, 346: 737–739
28 An Z S, Liu T, Lu Y, et al. The long-term paleomonsoon variation recorded by the loess-paleosol sequence in central China. Quat Int, 1990, 7: 91–95
29 An Z S, Kutzbach J E, Prell W L, et al. Evolution of Asian monsoons and phased uplift of the Himalaya–Tibetan Plateau since Late Miocene times. Nature, 2001, 411: 62–66
30 Hao Q, Wang L, Oldfield F, et al. Delayed build-up of Arctic ice sheets during 400000-year minima in insolation variability. Nature, 2012, 490: 393–396
31 Liu Q, Roberts A P, Larrasoaña J C, et al. Environmental magnetism: Principles and applications. Rev Geophys, 2012, 50: RG4002
32 Xie Y, Yuan F, Zhan T, et al. Geochemistry of loess deposits in northeastern China: Constraint on provenance and implication for disappearance of the large songliao palaeolake. J Geol Soc, 2017, 175: 146–162
33 Zeng L, Lu H, Yi S, et al. Long-term Pleistocene aridification and possible linkage to high-latitude forcing: New evidence from grain size and magnetic susceptibility proxies from loess-paleosol record in northeastern China. Catena, 2017, 154: 21–32
34 Guo Z T, Berger A, Yin Q Z, et al. Strong asymmetry of hemispheric climates during MIS-13 inferred from correlating China loess and Antarctica ice records. Clim Past, 2009, 5: 21–31
35 Chu B J, Gao Z C, Yang S S, et al. Quaternary geology and enviroment of Heilongjiang Province, China (in Chinese). Beijing: Ocean Press, 1988 [初本君, 高振操, 杨世生, 等. 黑龙江省第四纪地质与环境. 北京: 海洋出版社, 1988]

Summary for “东北平原钻孔的磁性地层定年及松嫩古湖演化”

Magnetostratigraphic dating of a drill core from the Northeast Plain of China: Implications for the evolution of Songnen paleo-lake

Tao Zhan[1*], Fangming Zeng[2], Yuanyun Xie[3], Ye Yang[1], Junyi Ge[4], Yongfa Ma[1], Yunping Chi[3], Chunguo Kang[5], Xia Jiang[6], Zhongyuan Yu[7], Jun Zhang[1], E Li[1] & Xin Zhou[8]

[1] *General Institute of Ecological Geology Survey and Research of Heilongjiang Province, Harbin 150030, China;*
[2] *Qinghai Institute of Salt Lakes, Chinese Academy of Sciences, Xining 810008, China;*
[3] *College of Geographic Science, Harbin Normal University, Harbin 150025, China;*
[4] *Institute of Vertebrate Paleontology and Paleoanthropology, Chinese Academy of Sciences, Beijing 100044, China;*
[5] *Geography Department, Harbin Institute, Harbin 150086, China;*
[6] *Heilongjiang Bureau of Geology & Mineral Resources, Harbin 150036, China;*
[7] *Comprehensive Disaster Mitigation Centre, Institute of Disaster Prevention, Sanhe 065201, China;*
[8] *School of Earth and Space Sciences, University of Science and Technology of China, Hefei 230026, China*
*Correspongding author, E-mail: hljzhantao@163.com

Lacustrine sediments from the Northeast Plain of China are an ideal archive for recording the climatic history and variability of the East Asian monsoon during the Quaternary in mid-latitude East Asia. However, the lack of a high-resolution stratigraphy and high-precision geochronology of these sediments has limited our understanding of the mechanisms of Quaternary climatic and environmental changes in the region. In this study, we present a high-resolution magnetic susceptibility stratigraphy and precise paleomagnetic and optically stimulated luminescence (OSL) chronologies for core Qiananlingzi (QAL) from the Northeast Plain. Paleomagnetic data were obtained using alternating-field (AF) demagnetization with a peak AF of 80 mT and increments of 2.5−10 mT. In addition, OSL dating was conducted on coarse-grained quartz (90−150 μm) using the single aliquot regenerative dose (SAR) protocol. Correlation of the recognized polarity intervals of the QAL core to the geomagnetic polarity timescale was achieved by combining the magnetostratigraphic and OSL geochronologic data. The results indicate that the sedimentary sequence spans the interval from the Olduvai normal subchron to the end of the Brunhes normal chron. According to the lithology and the magnetic susceptibility record, the core can be divided into four intervals, from bottom to top: the Qian'an Formation (fluvial yellow-green, brown-red and grey-brown silty sand, interbedded with brown-black silty clay, with gravel layers in the lower part); the Lingzi Formation and Lindian Formation (lacustrine grey-green clay interbedded with grey-white silty sand, with fossil bivalves); and a loess-like soil (predominantly brown-yellow clayey silt, alternating with fluviolacustrine grey-white, brown and black clay). The magnetic susceptibilities (MS) of the sediments of the lower fluvial Qian'an Formation and upper loess-like soil strata are generally higher, indicating the neoformation of strongly magnetic minerals under predominantly oxidizing conditions. By contrast, lower MS values occur in the lacustrine sediments of the Lingzi Formation and Lindian Formation, which indicate a reducing environment. Overall, the MS record of the QAL core exhibits clear orbital-scale variations, with higher MS values in coarse-grained silt layers, and lower values in fine-grained clay layers. After the application of a 300 mT DC field, the isothermal remanence (IRM) is only 70%, and a hysteresis loop remained unclosed at 500 mT. These characteristics indicate the substantial presence of high-coercivity magnetic minerals in the intervals with low MS values. Thermomagnetic measurements (χ-T) curves show an abrupt decrease in the heating curve at 580°C, indicating that magnetite is the dominant magnetic mineral, and a further decrease above 580°C indicates the presence of hematite. After the application of an applied DC field of 300 mT, the IRM reached 90%, the hysteresis loop was closed, and the heating limb of the χ-T curve did not decrease significantly after 580°C, indicating that low-coercivity magnetic minerals contributed substantially to the magnetic properties within the intervals of higher MS. The lacustrine sediments of the core were dated to ~1180–450 ka based on paleomagnetic and QSL dating, and interpolation of the age-depth relationship suggests that Songnen paleo-lake existed for ~730 ka. The grain-size record of the loess in the northeastern monsoon region shows no evidence of drought events at 450 ka, and records of MS and FeD/FeT from the deposits of the loess Plateau indicate a trend of increasing summer monsoon precipitation at this time. Therefore, the disappearance of the paleo-lake may be related to the multiple episodes of subsidence of the Yishu fault, which caused a diversion of the discharge of the Songhua River from the Songnen paleo-lake to the Sanjiang Plain. The high-resolution MS record and the precise chronology obtained in this study indicate that the lacustrine sedimentary sequence of QAL core can potentially resolve orbital-scale paleoclimate changes during the middle Pleistocene in mid-latitude East Asia. The Mid-Pleistocene Transition (MPT) is one of the most important climatic events in Quaternary paleoclimatology, and it is necessary to understand the response of different climatic systems to the MPT. Detailed environmental magnetic, sedimentological and geochemical studies of lacustrine sedimentary strata in the Northeast Plain in China should be carried out to explore the paleoclimatic record of the area, including the regional climatic response to the MPT.

Northeast Plain, Quaternary Songnen paleo-lake, magnetostratigraphy, optically stimulated luminescence, magnetic susceptibility

doi: 10.1360/N972018-01212